
Environmental factors affecting maerl bed structure in Brittany (France)

Dutertre Mickael^{1,*}, Grall Jacques², Ehrhold Axel³, Hamon Dominique¹

¹ IFREMER, ODE/DYNECO/Laboratoire Écologie Benthique, Technopôle Brest-Iroise, B.P. 70, 29280 Plouzané, France

² Institut Universitaire Européen de la Mer, UMS 3113, Observatoire Domaine Côtier, 29280 Plouzané, France

³ IFREMER, REM/GM/Laboratoire Environnements Sédimentaires, Technopôle Brest-Iroise, B.P. 70, 29280 Plouzané, France

* Corresponding author : Mickael Dutertre, email address : mickael.dutertre@yahoo.fr

Abstract :

This study used a large spatial scale approach in order to better quantify the relationships between maerl bed structure and a selection of potentially forcing physical factors. Data on maerl bed structure and morpho-sedimentary characteristics were obtained from recent oceanographic surveys using underwater video recording and grab sampling. Considering the difficulties in carrying out real-time monitoring of highly variable hydrodynamic and physicochemical factors, these were generated by three-dimensional numerical models with high spatial and temporal resolution. The BIOENV procedure indicated that variation in the percentage cover of thalli can best be explained (correlation = 0.76) by a combination of annual mean salinity, annual mean nitrate concentration and annual mean current velocity, while the variation in the proportion of living thalli can best be explained (correlation = 0.47) by a combination of depth and mud content. Linear relationships showed that the percentage cover of maerl thalli was positively correlated with nitrate concentration ($R^2 = 0.78$, $P < 0.01$) and negatively correlated with salinity ($R^2 = 0.81$, $P < 0.01$), suggesting a strong effect of estuarine discharge on maerl bed structure, and also negatively correlated with current velocity ($R^2 = 0.81$, $P < 0.01$). When maerl beds were deeper than 10 m, the proportion of living thalli was always below 30% but when they were shallower than 10 m, it varied between 4 and 100%, and was negatively correlated with mud content ($R^2 = 0.53$, $P < 0.01$). On the other hand, when mud content was below 10%, the proportion of living thalli showed a negative correlation with depth ($R^2 = 0.84$, $P < 0.01$). This large spatial scale explanation of maerl bed heterogeneity provides a realistic physical characterization of these ecologically interesting benthic habitats and usable findings for their conservation and management.

Keywords : Benthic habitats, Brittany, environmental factors, estuary, large spatial scale, maerl

1. Introduction

Maerl beds refer to intricate benthic habitats constituted by accumulations of living and dead unattached thalli of coralline algae which occur in tropical, temperate and polar environments (Bosence, 1983; Freiwald & Henrich, 1994). In European waters, most of them are patchily distributed and found at less than 30 m deep, except in the Mediterranean Sea where they can be found down to 100 m (Jacquotte, 1962; Birkett *et al.*, 1998; Hall-Spencer, 1998; De Grave *et al.*, 2000; Foster, 2001). Although this geographical distribution seems to be mainly constrained by the ecological requirements of the species constituting European maerl beds, such as *Phymatolithon calcareum* (Pallas) W.H. Adey & D.L. McKibbin and *Lithothamnium corallioides* (P.L. Crouan & H.M. Crouan) P.L. Crouan & H.M. Crouan, only a few studies have investigated the relationships between environment and physiological responses in these species, resulting in very variable conclusions about their ecological niches (Adey & McKibbin, 1970; Hall-Spencer & Moore, 2000; Wilson *et al.*, 2004; Martin *et al.*, 2006; 2007a; 2007b). Furthermore, although the morpho sedimentary environment of maerl beds can be clearly established by field samplings, the effect of the highly-variable hydrodynamics and physico-chemical properties of the water column may be misinterpreted due to the difficulty of carrying

74 out real-time monitoring, especially in temperate coastal ecosystems subject to a
75 semi-diurnal tidal cycle, freshwater outflows and a seasonal cycle (Barbera *et al.*,
76 2003; Wilson *et al.*, 2004; Dutertre *et al.*, 2013). The development of three-
77 dimensional environmental models generating continuous data on the variability of a
78 large variety of environmental factors, including hydrodynamic conditions and
79 physico-chemical properties (Cugier & Le Hir, 2002; Ménesguen *et al.*, 2007), can
80 therefore greatly improve the identification of environmental factors responsible for
81 the existence, structure and spatial distribution of benthic habitats such as maerl
82 beds (Warwick & Uncles, 1980; Gogina & Zettler, 2010; Dutertre *et al.*, 2013).

83 Accumulations of calcified thalli result in a large number of microhabitats
84 (microniches) formed by the space between branched forms together with hard
85 calcareous surfaces. Such complexity is characterized by a high diversity and density
86 of macrofaunal and algal species (Birkett *et al.*, 1998; Barbera *et al.*, 2003; Steller *et*
87 *al.*, 2003; Grall *et al.*, 2006; Hall-Spencer *et al.*, 2008; Peña & Bárbara, 2008; 2010;
88 Dutertre *et al.*, 2013). Maerl beds also provide nursery grounds of importance for
89 commercial species of fish and shellfish (Hall-Spencer *et al.*, 2003; Steller *et al.*,
90 2003). Being hot-spots of biodiversity and considered as a non-renewable resource
91 due to the slow growth rate of the thalli (Wilson *et al.*, 2004), maerl beds are a priority
92 of the European conservation policies, in particular when being massively extracted
93 to provide calcareous products for soil conditioning, water filtration systems,
94 cosmetics and also for the oil industry (Barbera *et al.*, 2003). The species richness
95 and density of the associated biodiversity are strongly dependent on the three-
96 dimensional structure of the maerl beds corresponding to the density and morphology
97 of thalli, the heterogeneity of the constituent particles (coexistence of fine particles
98 with large maerl thalli), and on the proportion of living thalli (Steller *et al.*, 2003;

99 Sciberras *et al.*, 2009; Meihoub Berlandi *et al.*, 2012). In spite of the ecological
100 influence of the structural heterogeneity of maerl beds, few data are available about
101 its determinism and evolution. Thus, although water motion, sedimentation and some
102 human activities have been considered driving factors of the variations in morphology
103 and vitality of maerl (Scoffin *et al.*, 1985; Steller & Foster, 1995; Marrack, 1999;
104 Barbera *et al.*, 2003), no clear quantitative relationships have been established
105 between environmental factors and maerl bed structure. In order to understand better
106 how the structure of maerl beds differs between them and how it may change with
107 time, a clear quantification of the influence of environmental factors forcing maerl bed
108 structure now appears necessary (Barbera *et al.*, 2003; Grall & Hall-Spencer, 2003;
109 Przeslawski *et al.*, 2011). Such quantification, essential for the development of
110 management tools such as habitat modelling, can be accomplished by a large spatial
111 scale approach, enabling the elimination of local misinterpretations by comparing
112 distant sites and, therefore, a more realistic physical characterization of benthic
113 habitats, as well as a discrimination between human and natural effects (Ellis &
114 Schneider, 2008; Dutertre *et al.*, 2013).

115 The aim of this study was to investigate and quantify relationships between
116 variations in maerl bed structure and a selection of potentially-forcing physical factors
117 in order to provide a consistent baseline for conservation and management
118 purposes. This was performed by integrating local structural data regarding the maerl
119 beds of Brittany, which are some of the most extensive in Europe, into a large spatial
120 scale approach. Maerl bed structure was described from data on the percent cover of
121 maerl thalli and the proportion of living thalli which were recently obtained using a
122 combination of underwater video-recordings and grab samplings. Quantitative
123 relationships between maerl bed structure and environmental factors were

124 determined using hydrodynamic and physico-chemical variables generated by three-
125 dimensional numerical models in order to better integrate their high spatio-temporal
126 variability.

127

128 **Materials and methods**

129

130 *Remote sensing and sampling strategy*

131

132 Within the framework of the French program REBENT (“Réseau Benthique”)
133 and the European Water Framework Directive, the physical structure of five maerl
134 beds of the Brittany coast was investigated by IFREMER (French Research Institute
135 for Exploration of the Sea) using a combination of remote sensing systems,
136 underwater video-recordings and grab samplings. The maerl beds of Paimpol and
137 Molène were investigated in 2008, while those of Glénan, Trévignon and Belle-Ile
138 were investigated in 2009 (Figure 1). A digital sidescan sonar EDGETECH DF-
139 1000[®], towed by the coastal vessel THALIA, was first used to carry out acoustic
140 profiles in order to identify maerl beds amongst the other morpho-sedimentary units,
141 while geographic locations were determined by a differential Global Positioning
142 System THALES AQUARIUS[®]. Sediment samplings and underwater video-
143 recordings were then performed within the areas where maerl beds had been
144 identified on acoustic profiles (Table 1). Sediment samples were collected with a
145 0.042 m² Shipek grab deployed from the coastal vessel THALIA, put into plastic bags
146 and frozen during their storage. In the laboratory, about 300 g of each sediment
147 sample was first wet-sieved using a 50- μ m stainless steel sieve. The fraction above

148 50 μm was dry-sieved on a sieve shaker, using a range of stainless steel sieves
149 placed at -4 phi intervals, down to 4 phi (63 μm). The retained fractions were weighed
150 in order to give a full particle size distribution and GRADISTAT 4.0 software was
151 used to calculate the mud content of the distribution, which corresponds to the
152 percentage of particles smaller than 63 μm . Living and dead maerl thalli were
153 included in sedimentary analysis. Underwater video-recordings were made using a
154 KONSBURG OE1372A-003 high-resolution colour video camera, equipped with a
155 waterproof projector and mounted on a metallic support in order to have a constant
156 distance between the camera and the surface of the maerl bed. The video camera
157 was towed by the coastal vessel THALIA above the maerl beds and dropped down
158 randomly near sediment sampling sites in order to obtain ten 0.160 m² photoquadrats
159 of the bottom.

160 In 2010, the European Institute for Marine Studies (IUEM) investigated the
161 physical structure of the maerl beds of Rade de Brest and Camaret (Figure 1). Within
162 each maerl bed, random sediment samplings were performed with a 0.100 m² Smith
163 McIntyre grab and then processed using the method described above (Table 1).
164 However, these investigations did not include underwater video-recordings.

165

166 *Analysis of the physical structure of the maerl beds*

167

168 The physical structure of the maerl beds was characterized by the percent
169 cover of maerl thalli (live + dead) determined *in situ* and the proportion of living thalli
170 determined in the laboratory. The percent cover of maerl thalli (live + dead) was
171 estimated by superimposing a 20×20 cm square grid on drop-down still images of the

172 maerl beds in order to determine the percentage of the seabed covered by maerl.
173 Due to the difficulty of distinguishing between living and dead thalli in the field, the
174 proportion of living thalli was estimated in the laboratory from the grab samples used
175 for the sedimentary analysis. According to their marked coloration, varying from
176 reddish-pink to reddish-purple, all the living thalli sampled in grab were separated
177 from the rest of the sediment (including dead thalli) and deposited on a 10×10 square
178 grid corresponding to the area of seabed sampled by the grab (0.042 m² and 0.100
179 m² for the Shipek and Smith McIntyre grab samples, respectively) in order to
180 determine the proportion of living thalli (i.e. the number of the sub-squares filled by
181 living thalli on the grid) on the seabed. Except for the subarea R16 of the maerl bed
182 of Rade de Brest where the seabed was 100 % covered by maerl stacks, the amount
183 of living thalli has never exceeded the size of the grid used to determine the
184 proportion of living thalli. While the proportion of living thalli was determined for each
185 sampling station of the seven maerl beds (Belle-Ile, Trévignon, Glénan, Camaret,
186 Rade de Brest, Molène and Paimpol), the percent cover of maerl thalli was not
187 determined for the maerl beds of Rade de Brest and Camaret due to the lack of drop-
188 down still images. *P. calcareum* and *L. corallioides* have been reported as the
189 dominant maerl-forming species in Brittany (Grall & Hall-Spencer, 2003), however, as
190 visual inspection of the thalli cannot enable a reliable taxonomic identification of the
191 maerl species, thalli were considered as if they belonged to the same maerl species.
192 Nevertheless, visual inspection enables a qualitative description of the relative thallus
193 morphology taking into account the shape and the branching pattern.

194

195 *Three-dimensional environmental models*

196

197 The MARS 3D (Three Dimensional Model for Applications at Regional Scale)
198 model has been developed by IFREMER to provide realistic descriptions of spatial
199 and temporal variations in coastal hydrodynamics (Ménèsquen *et al.*, 2007; 2014;
200 Lazure & Dumas, 2008). It uses regular orthogonal grids with square meshes,
201 aligned with geographic axes, in the horizontal plane. For each mesh, the water
202 column is divided into ten horizontal layers for which thickness is proportional to the
203 local water depth (σ -coordinates). Mechanical forcing of the MARS 3D
204 hydrodynamical model is made by barotropic sea-level oscillation at the oceanic
205 boundaries, and wind and atmospheric pressure at the sea surface (Arpege Model,
206 Météo-France). The salinity and temperature are calculated with a classic time
207 integration scheme. Flow rates of rivers such as Loire and Vilaine derive from
208 measured daily discharges. The ECOMARS 3D model, resulting from the coupling of
209 the MARS 3D model and a biochemical model, enables the description of spatial and
210 temporal variations in nutrient (nitrate, phosphate and silicate) concentrations and
211 oxygen saturation. River nutrient concentrations are computed from empirical
212 statistical relationships involving flow rate and time fitted. Suspended particulate
213 matter derives from satellite data and the suspended matter brought by the rivers,
214 which is simply simulated as a particulate conservative tracer. Oxygen saturation
215 derives from oxygen concentration measured in surface and bottom waters by buoys.
216 Environmental simulations generated by MARS 3D and ECOMARS 3D models have
217 been validated by numerous data from monitoring networks for the French coastal
218 zone (e.g. REPHY, MAREL, SOMLIT) and oceanographic cruises. Following the
219 recent development of the models in the framework of the PREVIMER project and
220 the possibility of having good validations by means of satellite observations and
221 seawater measurements, the year 2009 was chosen as the “reference” year to

222 generate hydrological variations because of the absence of exceptional climatic
223 events. For the maerl beds of Paimpol, Molène, Glénan, Trévignon and Belle-Ile,
224 temperature ($^{\circ}\text{C}$), salinity, oxygen saturation (%), suspended particulate matter
225 (SPM, mg.L^{-1}) and nutrients concentrations (nitrate and phosphate, μM) were
226 derived from the ECOMARS 3D-BRETAGNE model (resolution grid = 3 km, period =
227 12 h), while current velocity (m.s^{-1}) was obtained from the MARS 3D-MANGA
228 (MANche-GAScogne) model (resolution grid = 3 km, period = 1 h). For the maerl
229 beds of Rade de Brest and Camaret, the physico-chemical properties of the water
230 column were derived from the ECOMARS 3D-BRETAGNE zoom FINIS model
231 (resolution grid = 500 m, period = 12 h), while current velocity (m.s^{-1}) was obtained
232 from the MARS 3D-MANGA model zoom IROISE (resolution grid = 150 m, period = 1
233 h).

234 In its operational configuration, the WAVEWATCH III model is a wind-wave
235 model using unstructured grids with adaptive time stepping, which has been adapted
236 to be interfaced with ocean and atmospheric circulation models (Tolman, 2002;
237 Ardhuin *et al.*, 2014). Wave simulations have been extracted on regular grids for the
238 year 2009 and validated by numerous data from buoys, satellite observations and
239 oceanographic cruises. For all the maerl beds, significant wave agitation (m.s^{-1}) was
240 derived from the WAVEWATCH III ® NORGAS-UG (Nord-Gascogne-Unstructured
241 Grid) model (resolution grid = 200 m, period = 3 h).

242 Temporal and spatial variations in hydrological factors (temperature, salinity,
243 oxygen saturation, SPM concentration, nitrate concentration, current velocity and
244 significant wave agitation) were generated over all the year 2009 using the MARS 3D
245 and WAVEWATCH III environmental models in their operational configurations
246 implemented within the framework of the PREVIMER project (Dumas *et al.*, 2014).

247 For each hydrological factor, annual descriptive statistics (mean, standard deviation,
248 maximum and minimum) were calculated from the continuous temporal data
249 generated at the horizontal bottom layer of the water column, representing 1/10th of
250 the local water depth, in each mesh of the resolution grid covering a part of the maerl
251 beds. Annual standard deviation was used as an indicator of environmental
252 variability.

253

254 *Statistical analysis*

255

256 Seabed areas covered by the maerl beds of Paimpol, Molène, Glénan,
257 Trévignon and Belle-Ile, were virtually subdivided into geographical subareas
258 according to the 3×3 km meshes of the resolution grid of the MARS 3D model (Table
259 1). For these maerl beds, the percent cover of maerl thalli, proportion of living thalli,
260 depth, mud content and wave agitation were therefore averaged within each subarea
261 corresponding to a MARS 3D model's mesh. For the maerl beds of Rade de Brest
262 and Camaret, each subarea corresponded to a single sampling station and to a
263 single 0.5×0.5 MARS 3D model's mesh (Table 1).

264 The BIOENV procedure, implemented in the PRIMER[®] V6 software package,
265 was used to identify which combination of the tested environmental variables (mud
266 content, depth and the annual descriptive statistics of the hydrological factors
267 generated by the numerical models) best explained variations in maerl bed structure
268 (Clarke & Ainsworth, 1993). The results of the BIOENV procedure were illustrated by
269 a parallel display of nonmetric multidimensional scaling (NMDS) ordinations of the
270 subareas based on each structural component (percent cover of maerl thalli and
271 proportion of living thalli) of the maerl beds (Bray-Curtis dissimilarities) and the

272 associated best subset of explanatory environmental variables (Euclidean
273 dissimilarities). Non-parametric Spearman tests, implemented in Sigmastat 3.1
274 software, were also used to determine correlations between environmental
275 predictors. Finally, after checking the normality and homoscedasticity of the
276 distributions, linear regressions were used to describe the relationships between
277 maerl bed structure and selected environmental variables.

278

279 **Results**

280

281 *Structural description of the maerl beds*

282

283 The total areas of the Brittany maerl beds, which were then virtually subdivided
284 into subareas according to the resolution grids of the MARS 3D model, varied
285 between 1.9 and 23.0 km² (Table 1).

286 The maerl bed of Belle-Ile corresponded to a single subarea (B) where the
287 seabed was 92.5 ± 14.5 % covered by maerl thalli, while the proportion of living thalli
288 was 23.4 ± 15.5 %. Most of the thalli were characterized by short branches, while few
289 of them exhibited spherical shapes (Figure 2). Underwater video-recordings showed
290 that living thalli were mainly concentrated in hollows of megaripples generated by
291 wave action.

292 The maerl bed of Trévignon was subdivided into two subareas (T1 and T2).
293 Within T1, the percent cover of maerl thalli was 73.8 ± 11.3 %, while the proportion of
294 living thalli was 38.3 ± 13.0 %. Within T2, the seabed was 96.9 ± 18.3 % covered by
295 maerl thalli, while the proportion of living thalli was 83.0 ± 16.4 %. Thalli were

296 characterized by short branches within T1 (Figure 3), while they exhibited more
297 ramified morphotypes with longer branches within T2 (Figure 4).

298 The maerl bed of Glénan was subdivided into two subareas (G1 and G2). The
299 percent cover of maerl thalli was 78.5 ± 10.6 % within G1 and 68.5 ± 23.3 % within
300 G2. Grab samplings showed 10.0 ± 8.4 % of living thalli within G1 and 16.5 ± 10.6 %
301 of living thalli within G2. Within G1 and G2, thalli were relatively small and poorly
302 ramified (Figures 5-6).

303 The maerl bed of Molène was subdivided into two subareas (M1 and M2).
304 Within M1, the seabed was 71.0 ± 34.4 % covered by maerl thalli, while the
305 proportion of living thalli was 80.5 ± 27.5 %. Within M2, the seabed was 66.8 ± 7.2 %
306 covered by thalli, while the proportion of living thalli was 21.6 ± 16.9 %. Ramified
307 thalli were observed within each subarea of the maerl bed of Molène; however, within
308 M2, they were associated with sub-discoidal morphotypes with warty protuberances
309 (Figures 7-8).

310 The maerl bed of Paimpol was subdivided into three subareas (P1, P2 and P3).
311 The covering of the seabed by thalli within P1, P2 and P3 was 39.3 ± 15.7 %, $42.2 \pm$
312 28.6 % and 59.1 ± 29.6 %, respectively. The proportion of living thalli within P1, P2
313 and P3 was 28.6 ± 9.5 %, 24.4 ± 18.4 % and 37.5 ± 26.2 %, respectively. Highly
314 abraded sub-spheroidal thalli with warty protuberances were the dominant
315 morphotype within P1 (Figure 9), while they were mixed with nodulus and branched
316 ones within P2 (Figure 10). Within P3, branched thalli were clearly dominant (Figure
317 11).

318 For the maerl beds of Rade de Brest and Camaret, each sampling station
319 corresponded to a single subarea. On the whole, the proportion of living thalli varied
320 between 16.0 ± 12.4 and 100.0 ± 0 % within the maerl beds of Rade de Brest, while it

321 varied between 0.8 ± 0.2 and 28.3 ± 17.4 % within that of Camaret. Within Rade de
322 Brest and Camaret, thalli exhibited branched forms (Figures 12-13).

323

324 *Environmental setting of the maerl beds*

325

326 Within the maerl beds of the Brittany coast mud content varied between 0 and
327 46.6 % (Table 2). The highest mud content was found within the maerl beds of Rade
328 de Brest (average mud content = 28.6 ± 12.5 %) and Camaret (average mud content
329 = 7.9 ± 7.4 %), while other maerl beds developed on sediment with less than 2 % of
330 mud. The maerl beds of the Brittany coast were found between 0.7 and 25.9 m deep.
331 The shallowest maerl beds developed within the Rade de Brest, between 0.7 and 6.8
332 m, while the deepest developed at Paimpol, between 10.8 and 25.9 m (Table 2).

333 The Brittany maerl beds were found in areas characterized by an annual mean
334 current velocity varying between 0.02 and $0.73 \text{ m}\cdot\text{s}^{-1}$ (Table 2). The lowest values
335 were found at Trévignon (T2) and the highest at Paimpol (P1), where the maximum
336 reached $1.71 \text{ m}\cdot\text{s}^{-1}$. On the other hand, the annual mean wave agitation was lowest
337 at Paimpol ($P3 = 0.19 \pm 0.15 \text{ m}\cdot\text{s}^{-1}$) and highest at Belle-Ile ($B = 0.62 \pm 0.49 \text{ m}\cdot\text{s}^{-1}$),
338 where the maximum was $3.56 \text{ m}\cdot\text{s}^{-1}$.

339 The maerl beds of the Brittany coast were found in areas characterized by
340 annual mean water temperatures varying between 12.2 and 13.6°C , calculated for
341 Rade de Brest and Belle-Ile, respectively, while the lowest winter value was 3.9°C ,
342 calculated for Rade de Brest (Table 3). Annual mean salinity was highest at Paimpol
343 (35.3) and lowest at Rade de Brest (31.9) which showed the lowest annual value
344 (24.5) (Table 3). Annual mean suspended particulate matter (SPM) concentration
345 varied between 0.5 and $2.2 \text{ mg}\cdot\text{L}^{-1}$, while annual mean nitrate concentration varied

346 between 3.3 and 41.0 μM (Table 3). Rade de Brest showed the highest nitrate
347 concentrations which could reach 148.2 μM (Table 3). Annual mean oxygen
348 saturation, varying between 92 and 100 %, appeared elevated for all the maerl beds
349 (Table 3). The lowest oxygen saturation was calculated for Trévignon, where the
350 summer value fell to 59 %.

351

352 *Relationships between maerl bed structure and environmental factors*

353

354 The BIOENV procedure indicated that the variations in the percent cover of
355 thalli can best be explained by a combination of three environmental variables
356 (correlation = 0.76). These corresponded to annual mean salinity, annual mean
357 nitrate concentration and annual mean current velocity, showing individually a
358 relatively high correlation with the percent cover of maerl thalli (correlation = 0.70,
359 0.64 and 0.62, respectively) compared to other environmental variables (correlation <
360 0.30). The NMDS ordinations based on the percent cover of maerl thalli and the best
361 subset of explanatory environmental variables (annual mean salinity, annual mean
362 nitrate concentration and annual mean current velocity), showed a relatively similar
363 arrangement of the subareas along a horizontal axis (especially for B, P1 and P2)
364 tending to respect their geographic distribution along the Brittany coast (Figures 14-
365 15). However, the subareas were separated into four distinct clusters in the NMDS
366 ordination based on the percent cover of maerl thalli (Figure 14), while only the
367 subareas corresponding to the maerl bed of Paimpol (P1, P2 and P3) were distinctly
368 separated from the others in the NMDS ordination based on the best subset of
369 explanatory environmental variables (Figure 15). The significance of these
370 relationships was revealed by linear relationships between the percent cover of maerl

371 thalli and annual mean salinity ($\log(\text{percent cover}) = -0.26 \times \text{annual mean salinity} +$
372 10.84 , $n = 10$, $R^2 = 0.81$, $p < 0.01$), annual mean nitrate concentration ($\log(\text{percent}$
373 $\text{cover}) = 0.06 \times \text{annual mean nitrate concentration} + 1.47$, $n = 10$, $R^2 = 0.78$, $p <$
374 0.01), and annual mean current velocity ($\log(\text{percent cover}) = -0.46 \times \text{annual mean}$
375 $\text{current velocity} + 1.97$, $n = 10$, $R^2 = 0.81$, $p < 0.01$) (Figures 18-20). Spatial variations
376 in annual mean salinity and annual mean nitrate concentration appeared to be
377 negatively correlated (Spearman correlation = -0.84 , $p < 0.01$). Annual mean current
378 velocity also showed some degree of correlation with annual mean salinity
379 (Spearman correlation = 0.61 , $p < 0.01$) and annual mean nitrate concentration
380 (Spearman correlation = -0.68 , $p < 0.01$). For the maerl beds of Belle-Ile, Trévignon,
381 Glénan, Molène and Paimpol, there was no significant relationship between the
382 percent cover of maerl thalli and the proportion of living thalli (Spearman correlation =
383 0.13 , $p = 0.68$).

384 As revealed by the BIOENV procedure, the variations in the proportion of living
385 thalli can best be explained by the combination of depth and mud content (correlation
386 = 0.47). These two environmental variables showed individually higher correlations
387 (correlation = 0.36 and 0.23 for depth and mud content, respectively) with the
388 proportion of living thalli than the others (correlation < 0.18). The NMDS ordinations
389 based on the proportion of living thalli and the best subset of explanatory
390 environmental variables (depth and mud content) tended to separate the subareas of
391 the shallow maerl bed of Rade de Brest (R1 - R18, depth < 6.8 m) from those of the
392 the deeper maerl bed of Camaret (C1 - C10, depth > 13.6 m) (Figures 16-17).
393 Similarly, the shallow subarea (T2, depth = 6.1 m) of the maerl bed of Trévignon was
394 separated from the deeper subarea (T1, depth = 14.1 m) in the NMDS ordinations.
395 For the maerl bed of Rade de Brest, where the range of mud content was the largest

396 (2.7 - 46.6 %), NMDS ordinations separated also the subareas showing the lowest
397 mud content (R1, R15 and R16, mud content < 10 %) from those showing the highest
398 mud content (R4, R5, R6, R7 and R13, mud content > 40 %), independently from the
399 depth. For the maerl bed of Camaret, NMDS ordinations based on the proportion of
400 living thalli and the best subset of explanatory environmental variables also showed a
401 relatively good match for the muddiest subareas (C1, C6, C9 and C10, mud content
402 > 10 %), independently from the depth. Although mud content showed an overall
403 correlation with depth (Spearman correlation = - 0.65, $p < 0.01$), these two
404 environmental variables were not significantly correlated for a depth less than 10 m
405 (Spearman correlation = - 0.15, $p = 0.52$). For subareas deeper than 10 m, proportion
406 of living thalli was always lower than 30 % while for subareas at less than 10 m, it
407 varied between 4 and 100 % and showed a significant linear relationship with mud
408 content (Figure 21, $\log(\text{proportion of living thalli}) = - 0.01 \times \text{mud content} + 2.03$, $n =$
409 20 , $R^2 = 0.53$, $p < 0.01$). In this case, the proportion of living thalli progressively
410 decreased when mud content increased from 0 to 46.6 %. On the other hand, for
411 mud content lower than 10 %, the proportion of living thalli showed a significant linear
412 relationship with depth (Figure 22, $\log(\text{proportion of living thalli}) = - 0.05 \times \text{depth} +$
413 2.11 , $n = 15$, $R^2 = 0.84$, $p < 0.01$). Being strongly affected by human exploitation (see
414 below), the proportions of living thalli within the maerl bed of Glénan (subareas G1
415 and G2) were not used to establish the linear relationships.

416

417 **Discussion**

418

419 *Influence of estuarine outputs on the percent cover of maerl thalli*

420

421 Within the maerl beds of the Brittany coast, the percent cover of maerl thalli
422 appeared to be strongly related to spatial variations in both salinity and nitrate
423 concentration. In fact, from the eastern part of Southern Brittany to the eastern part of
424 Northern Brittany, the percent cover of maerl thalli decreased simultaneously with the
425 increase in annual mean salinity and the decrease in annual mean nitrate
426 concentration. Spatial variations in these two environmental variables are strongly
427 driven by regular estuarine outputs from the Vilaine and Loire estuaries, situated in
428 the eastern part of Southern Brittany, which generate a marked east-west gradient
429 between riverine-influenced waters and oceanic-influenced waters (Dutertre *et al.*,
430 2013). Simulations from the three-dimensional environmental models, as well as
431 remote sensing observations, showed that the attenuated effects of plumes from both
432 these rivers can also be detected as far as the Molène Archipelago during winter
433 (December-February) floods. On the other hand, small rivers situated along the
434 Brittany coast generate slightly decreasing gradients of estuarine conditions with
435 distance from the shore. In Northern Brittany, the maerl bed of Paimpol was not
436 affected by the estuarine outputs and was therefore subject to the lowest annual
437 mean nitrate concentration and the highest annual mean salinity. The influence of
438 estuarine outputs was clearly visible along the coastal fringe of Southern Brittany
439 where the highest percent cover - more than 92 % of the seabed covered - was found
440 at Belle-Ile, directly exposed to releases from the Loire and Vilaine Rivers, and at
441 Trévignon, situated near the mouths of small rivers of Concarneau Bay. In areas
442 adjacent to these maerl beds, the influence of estuarine outputs on benthic
443 ecosystems was confirmed by the presence of particular macrofaunal communities
444 (Glémarec, 1969; Dutertre *et al.*, 2013). Although these results demonstrate an
445 influence of estuarine outputs on the percent cover of maerl thalli, the individual

446 effect of riverine-influenced factors is difficult to distinguish because they co-vary.
447 The occurrence of European maerl beds near estuaries was formerly attributed to a
448 drop in salinity measured in surface waters (Joubin, 1910). However, experimental
449 studies appear necessary to understand how the spatial variations of the bottom
450 salinity observed in this study influence the percent cover of maerl thalli. On the other
451 hand, the data available about the nutrient fluxes in maerl communities found on
452 Rade de Brest (Martin *et al.* 2007b) suggest that nitrate concentration could be the
453 main riverine-influenced factor responsible for the variations in the percent cover of
454 maerl thalli along the Brittany coast. In the same way, in the sublittoral zone of south-
455 western Hokkaido, a positive relationship was experimentally demonstrated between
456 thallus growth of the coralline alga *Lithophyllum yessoense* and nitrate concentration
457 ranging from 0 to 10 μM (Ichiki *et al.*, 2000) while, in the present study, annual mean
458 nitrate concentration ranged from 3.32 to 8.16 μM . Taking into account the gradual
459 increase in the amount of nitrates released by rivers since the 1970's, especially in
460 relation to farming activities, their potential effect on maerl bed structure should be
461 considered for conservation and management purposes. Another potential influence
462 of estuarine outputs on the growth and reproduction of coralline algae constituting
463 maerl beds could be variations in calcium concentration (Martin *et al.*, 2006; 2007a).
464 In fact, available data suggest that calcium carbonates accumulated in the Loire
465 River are dissolved at the level of the estuary (Grosbois *et al.*, 2001), involving a
466 massive release of dissolved calcium which is probably spread by the river's plume.

467

468 *Influence of current velocity on the percent cover of maerl thalli*

469

470 The Brittany maerl beds are found in seabed areas where the current velocity
471 showed an annual mean varying from 0.02 to 0.73 m.s⁻¹, and a maximum reaching
472 1.71 m.s⁻¹. In these areas, the percent cover of maerl thalli appeared related to the
473 annual mean current velocity. The lowest percent cover - less than 59 % of the
474 seabed covered - was found within the Paimpol maerl bed, where the annual mean
475 current velocity is higher than 0.50 m.s⁻¹ whereas, within the other maerl beds, where
476 the annual mean current velocity is lower than 0.30 m.s⁻¹, the percent cover of maerl
477 thalli was higher than 66 %. Moreover, within the Paimpol maerl bed, the percent
478 cover of maerl thalli was higher in the more sheltered subareas (P2 and P3). The
479 strong relationship established between bottom current velocity and the percent
480 cover of maerl thalli is probably due to their transport by water current as
481 demonstrated in tropical reefs, where Scoffin *et al.* (1985) showed that individual
482 branched thalli moved when the tidal current velocity reached 0.30 - 0.40 m.s⁻¹. The
483 dispersion of thalli occurring above this threshold of hydrodynamics is consistent with
484 the lowest densities of maerl found within the maerl bed of Paimpol. Thus, the
485 dominance of abraded sub-spheroidal thalli with warty protuberances in this maerl
486 bed (Figures 9-11), as well as their presence in the maerl bed of Molène (Figures 7-
487 8), can be associated with abrasion generated by the movements of thalli during their
488 transport (Marrack, 1999).

489 Variations in both the percent cover and morphology of thalli can affect the
490 associated biodiversity of maerl beds (Steller *et al.*, 2003; Sciberras *et al.*, 2009;
491 Meihoub Berlandi *et al.*, 2012). For example, when thalli are sparse or non-branched,
492 maerl beds exhibit a less heterogeneous structure and contain less interstitial fauna.
493 However, variations in thallus morphology due to the diversity of coralline algal
494 species should also be considered. Although *P. calcareum* and *L. corallioides* are not

495 characterized by sub-spheroidal thalli and have been reported to be dominant in
496 Brittany maerl beds (Grall & Hall-Spencer, 2003), this dominance must be confirmed
497 by genetic studies.

498

499 *Environmental factors affecting the proportion of living thalli*

500

501 The proportion of living thalli in the maerl beds of the Brittany coast appeared
502 significantly linked to depth and mud content. The relationship with depth was clearly
503 highlighted by the fact that the proportion of living thalli was always lower than 30 %
504 in areas deeper than 10 m, while the highest proportions of living thalli were only
505 found at less than 10 m. On the other hand, at less than 10 m, the proportion of living
506 thalli was also affected by the amount of mud contained in the sediment. For this
507 depth range, the proportion of living thalli, which varied between 84 and 100 % when
508 sediment contained less than 10 % of mud, decreased simultaneously with the
509 increase in mud content. The effect of these two environmental variables on the
510 proportion of living thalli can be related to the diminution of light intensity, even
511 though the irradiance requirements of maerl species are not known and they are
512 generally considered as low-light adapted organisms (Birkett *et al.*, 1998; Wilson *et*
513 *al.*, 2004; Teichert *et al.*, 2012). The proportion of penetrating light is known to
514 decrease with depth, while silt deposition on thalli involves a smothering effect,
515 limiting their access to light and/or gaseous exchange (Steller & Foster, 1995; Hall-
516 Spencer, 1998; Hall-Spencer & Moore, 2000; Riul *et al.*, 2008). For example, the
517 burial of thalli resulting from the re-suspension of sediment by scallop dredging is
518 known to involve a reduction in living thalli of more than 70 %, with no sign of
519 recovery after four years (Wilson *et al.*, 2004). Thus, the disappearance between

1969 and 2009 of the maerl bed situated at the south of Quiberon Bay, where residual macrofaunal communities characterizing maerl habitat still subsist (Dutertre *et al.*, 2013), probably results from the silting of thalli due to increased shellfish dredging activities and oyster farming. Although turbidity can also affect the penetration depth of light, the simulations of three-dimensional environmental models and remote sensing observations revealed that the concentration of suspended particle matter was relatively low (annual mean SPM concentration $< 2.2 \text{ mg.L}^{-1}$) above the maerl beds. While Lemoine (1910) reported between 50 and 100 % of living thalli within the maerl bed of Glénan, the lower proportions of living thalli (< 20 %) observed now probably result from the huge exploitation which occurred during the second part of the twentieth century (Grall & Hall-Spencer, 2003; Hall-Spencer *et al.*, 2008). Indeed, the wash of extracted maerl involves a release of fine particles which deposit on the sea bottom and kill living maerl. The dominance of small poorly-branched thalli observed within the maerl bed of Glénan (Figures 5-6) can be also associated to fragmentation by dredging and extraction (Hall-Spencer & Moore, 2000).

536

537 *Implications for the conservation and management of the maerl beds*

538

539 The large spatial scale ecological approach implemented in this study provides
540 findings having significant implications for the conservation and management of the
541 ecologically interesting benthic habitats constituted by maerl beds. This approach
542 enables the detection of the influence of some important factors, such as estuarine
543 outputs, occurring at a wider spatial scale than that considered by local surveys
544 generally performed in marine benthic ecology. Moreover, while local environmental

545 conditions can lead to misinterpretations of benthic habitat characteristics at a small
546 spatial scale (Ellis & Schneider, 2008), site-to-site comparisons of the physical
547 environment reduce site-related artefacts and enable a more realistic environmental
548 setting of the maerl beds, including anthropogenic effects. More specifically, the
549 quantitative results provided by this study enable the determination of environmental
550 thresholds explaining the structural heterogeneity of maerl beds on which depends
551 the biological diversity associated with this habitat (Steller *et al.*, 2003; Sciberras *et*
552 *al.*, 2009; Meihoub Berlandi *et al.*, 2012). The non-explained part of this structural
553 heterogeneity can be therefore related to non-tested factors, including the impacts of
554 human activities such as fishing, aquaculture or extraction, which are often difficult to
555 quantify and distinguish from naturally-induced effects (Barbera *et al.*, 2003). Within
556 the framework of the implementation of conservation and management strategies of
557 the maerl beds, and of the improvement of benthic habitat modeling, such
558 quantifications are usable to understand better how the structure of maerl beds
559 differs between them and how it may change with time (Barbera *et al.*, 2003; Méléder
560 *et al.*, 2010).

561 The output from mathematical models may not fully represent the complex
562 functioning of the coastal environment and their use is dependent on the spatial and
563 time resolutions. Nevertheless, the significant relationships established between
564 maerl bed structure and physical factors suggest that, after validations by field data,
565 three-dimensional environmental models can be useful tools to support ecosystem
566 management in particular by enabling the generation of summary statistics to
567 quantify the effect of highly variable hydrological factors. In fact, numerical models
568 can generate continuous variations in a large variety of environmental factors, even
569 in marine areas where monitoring is not easy such as the sea bottom. Considering

570 the diversity of the environmental factors used and the reliability of the 3D models at
571 a large spatial scale (Ménesguen *et al.*, 2007), our results provide a good estimation
572 of the part of the structural heterogeneity of the maerl beds which can be explained
573 by the abiotic factors tested. However, as maerl beds are persistent in time and
574 constituted by long-lived maerl thalli (Barbera *et al.*, 2003), their structural
575 heterogeneity can also result from environmental changes (e.g. climate warming and
576 nutrient enrichment) and/or exceptional climatic events (e.g. storms) which occurred
577 over past years but cannot be correctly estimated with the models used in this study
578 due to the lack of consistent and reliable field validations for years prior to 2009.

579 Another important point to take into account when determining the
580 environmental influence on maerl beds is the taxonomic diversity of the maerl thalli.
581 For example, as it is difficult to distinguish dominant “maerl” species clearly without
582 histological observations or genetic analyses, maerl beds may be constituted by a
583 mix of different coralline algal species. Thus, although the ecological requirements of
584 each “maerl” species are still not clearly known, the relative proportion of these
585 species within a maerl bed could influence variations in the environmental setting of
586 maerl beds.

587

588 **Acknowledgements**

589

590 This work was jointly funded by IFREMER and the French Agency for Protected
591 Marine Areas (AAMP), which have also funded the French program REBENT
592 alongside Region Bretagne and the European Regional Development Fund
593 (FEDER). The authors wish to thank Philippe Cugier, Alain Ménesguen, and Fabrice
594 Lecornu, coordinator of the PREVIMER project, for the use of the 3D environmental

595 models. We also thank Xavier Caisey and Jean-Dominique Gaffet for their technical
596 assistance, as well as anonymous reviewers for their valuable comments on the
597 manuscript.

598

599 **References**

600

601 Adey, W.H. & McKibbin, D.L. (1970). Studies on the maerl species *Phymatolithon*
602 *calcareum* (Pallas) nov. comb. and *Lithothamnion corallioides* Crouan in the Ria
603 de Vigo. *Botanica Marina*, **13**: 100-106.

604 Arduin, F., Accensi, M., Roland, A., Girard, F., Filipot, J.-F., Leckler, F. & Le Roux,
605 J.-F. (2014). Numerical wave modeling in PREVIMER: multi-scale and multi-
606 parameter demonstrations. *Mercator Ocean - Quarterly Newsletter*, **49**: 39-43.

607 Barbera, C., Bordehore, C., Borg, J.A., Glémarec, M., Grall, J., Hall-Spencer, J.M.,
608 De la Huz, C., Lanfranco, E., Lastra, M. & Moore, P.G. (2003). Conservation
609 and management of northeast Atlantic and Mediterranean maerl beds. *Aquatic*
610 *Conservation: Marine and Freshwater Ecosystems*, **13**: S65-S76.

611 Birkett, D.A., Maggs, C.A. & Dring, M.J. (1998). Maerl (volume V). An overview of
612 dynamic and sensitivity characteristics for conservation management of marine
613 SACs. *Scottish Association for Marine Science (UK Marine SACs Project)*.

614 Bosence, D.W.J. (1983). The occurrence and ecology of recent rhodoliths - a review.
615 In T.M. Peryt (Editor), Coated Grains. *Springer-Verlag, Berlin*, 225-242.

616 Clarke, K.R. & Ainsworth, M. (1993). A method of linking multivariate community
617 structure to environmental variables. *Marine Ecology Progress Series*, **92**: 205-
618 219.

- 619 Cugier, P. & Le Hir, P. (2002). Development of a 3D hydrodynamic model for coastal
620 ecosystem modelling. Application to the plume of the Seine River (France).
621 *Estuarine, Coastal and Shelf Science*, **55**: 673-695.
- 622 De Grave, S., Fazakerley, H., Kelly, L., Guiry, M.D., Ryan, M. & Walshe, J. (2000). A
623 study of selected maerl beds in Irish waters and their potential for sustainable
624 extraction. *Marine Resource Series, No. 10. Marine Institute, Dublin*.
- 625 Dumas, F., Pineau-Guillou, L., Lecornu, F., Le Roux, J.-F. & Le Squère, B. (2014).
626 General introduction: previmer, a french pre-operational coastal ocean
627 forecasting capability. *Mercator Ocean - Quarterly Newsletter*, **49**: 3-8.
- 628 Dutertre, M., Hamon, D., Chevalier, C. & Ehrhold, A. (2013). The use of the
629 relationships between environmental factors and benthic macrofaunal
630 distribution in the establishment of a baseline for coastal management. *ICES*
631 *Journal of Marine Science*, **70**: 294-308.
- 632 Ellis, J.T. & Schneider, D.C. (2008). Spatial and temporal scaling in benthic ecology.
633 *Journal of Experimental Marine Biology and Ecology*, **366**: 92-98.
- 634 Foster, M.S. (2001). Rhodoliths: between rocks and soft places. *Journal of*
635 *Phycology*, **37**: 659-667.
- 636 Freiwald, A. & Henrich, R. (1994). Reefal coralline algal build-ups within the Arctic
637 Circle: morphology and sedimentary dynamics under extreme environmental
638 seasonality. *Sedimentology*, **41**: 963-984.
- 639 Glémarec, M. (1969). Les peuplements benthiques du plateau continental nord-
640 Gascogne. PhD thesis, Université de Paris.
- 641 Gogina, M. & Zettler, M.L. (2010). Diversity and distribution of benthic macrofauna in
642 the Baltic Sea. Data inventory and its use for species distribution modelling and
643 prediction. *Journal of Sea Research*, **64**: 313-321.

- 644 Grall, J. & Hall-Spencer, J.M. (2003). Problems facing maerl conservation in Brittany.
645 *Aquatic Conservation: Marine and Freshwater Ecosystems*, **13**: S55-S64.
- 646 Grall, J., Le Loc'h, F., Guyonnet, B. & Riera, P. (2006). Community structure and
647 food web based on stable isotopes ($\delta^{15}\text{N}$ and $\delta^{13}\text{C}$) analyses of a North
648 Eastern Atlantic maerl bed. *Journal of Experimental Marine Biology and*
649 *Ecology*, **338**: 1-15.
- 650 Grosbois, C., Négrel, P., Grimaud, D. & Fouillac, C. (2001). An overview of dissolved
651 and suspended matter fluxes in the Loire River basin: natural and
652 anthropogenic inputs. *Aquatic Geochemistry*, **7**: 81-105.
- 653 Hall-Spencer, J.M. (1998). Conservation issues concerning the molluscan fauna of
654 maerl beds. *Journal of Conchology Special Publication*, **2**: 271-286.
- 655 Hall-Spencer, J.M., Grall, J., Moore, P.G. & Atkinson, R.J.A. (2003). Bivalve fishing
656 and maerl-bed conservation in France and the UK – retrospect and prospect.
657 *Aquatic Conservation: Marine and Freshwater Ecosystems*, **13**: S33-S41.
- 658 Hall-Spencer, J.M., Kelly, J. & Maggs, C.A. (2008). Assessment of maerl beds in the
659 OSPAR area and the development of a monitoring program. Department of the
660 Environment, Heritage & Local Government (DEHLG), Ireland.
- 661 Hall-Spencer, J.M. & Moore, P.G. (2000). Scallop dredging has profound, long-term
662 impacts on maerl habitats. *ICES Journal of Marine Science*, **57**: 1407-1415.
- 663 Ichiki, S., Mizuta, H. & Yamamoto, H. (2000). Effects of irradiance, water temperature
664 and nutrients on the growth of sporelings of the crustose coralline alga
665 *Lithophyllum yessoense* Foslie (Corallinales, Rhodophyceae). *Phycological*
666 *Research*, **48**: 115-120.
- 667 Jacquotte, R. (1962). Étude des fonds de maërl de Méditerranée. *Recueil des*
668 *Travaux de la station marine d'Endoume*, **26**: 141-235.

- 669 Joubin, L. (1910). Recherches sur la distribution océanographique des végétaux
670 marins dans la région de Roscoff. *Annales de l'Institut Océanographique de*
671 *Monaco*, **1**: 1-17.
- 672 Lazure, P. & Dumas, F. (2008). An external–internal mode coupling for a 3D
673 hydrodynamical model for applications at regional scale (MARS). *Advances in*
674 *Water Resources*, **31**: 233-250.
- 675 Lemoine, P. (1910). Répartition et mode de vie du maërl (*Lithothamnium calcareum*)
676 aux environs de Concarneau (Finistère). *Annales de l'Institut océanographique*,
677 *Paris*, **1**: 1-29.
- 678 Marrack, E.C. (1999). The relationship between water motion and living rhodolith
679 beds in the southwestern Gulf of California, Mexico. *Palaeos*, **14**: 159-171.
- 680 Martin, S., Castets, M.D. & Clavier, J. (2006). Primary production, respiration and
681 calcification of the temperate free-living coralline alga *Lithothamnion*
682 *corallioides*. *Aquatic Botany*, **85**: 121-128.
- 683 Martin, S., Clavier, J., Chauvaud, L. & Thouzeau, G. (2007a). Community metabolism
684 in temperate maerl beds. I. Carbon and carbonate fluxes. *Marine Ecology*
685 *Progress Series*, **335**: 19-29.
- 686 Martin, S., Clavier, J., Chauvaud, L. & Thouzeau, G. (2007b). Community metabolism
687 in temperate maerl beds. II. Nutrient fluxes. *Marine Ecology Progress Series*,
688 **335**: 31-41.
- 689 Meihoub Berlandi, R., Figueiredo, M.A.O. & Paiva, P.C. (2012). Rhodolith
690 morphology and the diversity of polychaetes off the Southeastern Brazilian
691 Coast. *Journal of Coastal Research*, **28(1)**: 280-287.

- 692 Méléder, V., Populus, J., Guillaumont, B., Perrot, T. & Mouquet, P. (2010). Predictive
693 modelling of seabed habitats: case study of subtidal kelp forests on the coast of
694 Brittany, France. *Marine Biology*, **157**: 1525-1541.
- 695 Ménesguen, A., Dussauze, M., Lecornu, F., Dumas, F. & Thouvenin, B. (2014).
696 Operational modelling of nutrients and phytoplankton in the bay of Biscay and
697 English Channel. *Mercator Ocean - Quarterly Newsletter*, **49**: 87-92.
- 698 Ménesguen, A., Cugier, P., Loyer, S., Vanhoutte-Brunier, A., Hoch, T., Guillaud, J.-F.
699 & Gohin, F. (2007). Two- or three-layered box models versus fine 3D models for
700 coastal ecological modelling? A comparative study in the English Channel
701 (Western Europe). *Journal of Marine Systems*, **64**: 47-65.
- 702 Peña, V. & Bárbara, I. (2008). Maërl community in the north-western Iberian
703 Peninsula: a review of floristic studies and long-term changes. *Aquatic
704 Conservation: Marine and Freshwater Ecosystems*, **18**: 339-366.
- 705 Peña, V. & Bárbara, I. (2010). Seasonal patterns in the maërl community of shallow
706 European Atlantic beds and their use as a baseline for monitoring studies.
707 *European Journal of Phycology*, **45(3)**: 327-342.
- 708 Przeslawski, R., Currie, D.R., Sorokin, S.J., Ward, T.M., Althaus, F. & Williams, A.
709 (2011). Utility of a spatial habitat classification system as a surrogate of marine
710 benthic community structure for the Australian margin. *ICES Journal of Marine
711 Science*, **68**: 1954-1962.
- 712 Riul, P., Targino, C.H., Farias, J.N., Visscher, P.T. & Horta, P.A. (2008). Decrease in
713 *Lithothamnion* sp. (Rhodophyta) primary production due to the deposition of a
714 thin sediment layer. *Journal of the Marine Biological Association of the United
715 Kingdom*, **88**: 17-19.

- 716 Sciberras, M., Rizzo, M., Mifsud, J.R., Camilleri, K., Borg, J.A., Lanfranco, E. &
717 Schembri, P.J. (2009). Habitat structure and biological characteristics of a maerl
718 bed off the northeastern coast of the Maltese Islands (central Mediterranean).
719 *Marine Biodiversity*, **39**: 251-264.
- 720 Scoffin, T.P., Stoddart, D.R., Tudhope, A.W. & Woodroffe, C. (1985). Rhodoliths and
721 coralloliths of Muri Lagoon, Rarotonga, Cook Islands. *Coral Reefs*, **4**: 71-80.
- 722 Steller, D.L., Foster, M.S. (1995). Environmental factors influencing distribution and
723 morphology of rhodoliths in Bahía Concepción, B.C.S., Mexico. *Journal of*
724 *Experimental Marine Biology and Ecology*, **194**: 201-212.
- 725 Steller, D.L., Riosmena-Rodríguez, R., Foster, M.S. & Roberts, C.A. (2003).
726 Rhodolith bed diversity in the Gulf of California: the importance of rhodolith
727 structure and consequences of anthropogenic disturbances. *Aquatic*
728 *Conservation: Marine and Freshwater Ecosystems*, **13**: S5-S20.
- 729 Teichert, S., Woelkerling, W., Rüggeberg, A., Wisshak, M., Piepenburg, D.,
730 Meyerhofer, M., Form, A., Büdenbender, J. & Freiwald, A. (2012). Rhodolith
731 beds (Corallinales, Rhodophyta) and their physical and biological environment
732 at 80°31'N in Nordkappbukta (Nordaustlandet, Svalbard Archipelago, Norway).
733 *Phycologia*, **51(4)**: 371-390.
- 734 Tolman, H.L. (2002). Distributed-memory concepts in the wave model WAVEWATCH
735 III. *Parallel Computing*, **28**: 35-52.
- 736 Warwick, R.M. & Uncles, R.J. (1980). Distribution of benthic macrofauna associations
737 in the Bristol Channel in relation to tidal stress. *Marine Ecology Progress Series*,
738 **3**: 97-103.

739 Wilson, S., Blake, C., Berges, J.A. & Maggs, C.A. (2004). Environmental tolerances
740 of free-living coralline algae (maerl): implications for European maerl
741 conservation. *Biological Conservation*, **120**: 283-293.

742

743 Table 1. Subareas and associated number of sampling stations for the Brittany maerl
 744 beds. For each maerl bed, the total area and the materials used for the determination
 745 of maerl bed structure are indicated.

Maerl bed	Total area (km ²)	Subareas (number of sampling stations)	Materials
Belle-Ile	16.8	B(12)	Shipek grab samples Underwater video recordings
Trévignon	23.0	T1(2), T2(4)	Shipek grab samples Underwater video recordings
Glénan	5.2	G1(5), G2(2)	Shipek grab samples Underwater video recordings
Camaret	1.9	C1 – C10 (1 sampling station / subarea)	Smith-McIntyre grab samples
Rade de Brest	10.7	R1 – R18 (1 sampling station / subarea)	Smith-McIntyre grab samples
Molène	2.8	M1(11), M2(2)	Shipek grab samples Underwater video recordings
Paimpol	22.2	P1(5), P2(12), P3(5)	Shipek grab samples Underwater video recordings

746

747

748 Table 2. Morpho-sedimentary and hydrodynamic characteristics of the maerl beds of
 749 the Brittany coast. Mud content was measured in grab samples, while current velocity
 750 and wave agitation were generated near the bottom by three-dimensional numerical
 751 models. For current velocity and wave agitation, annual mean (bold characters) and
 752 annual maximum values are given, while annual minimum values are equal to 0 in all
 753 cases.

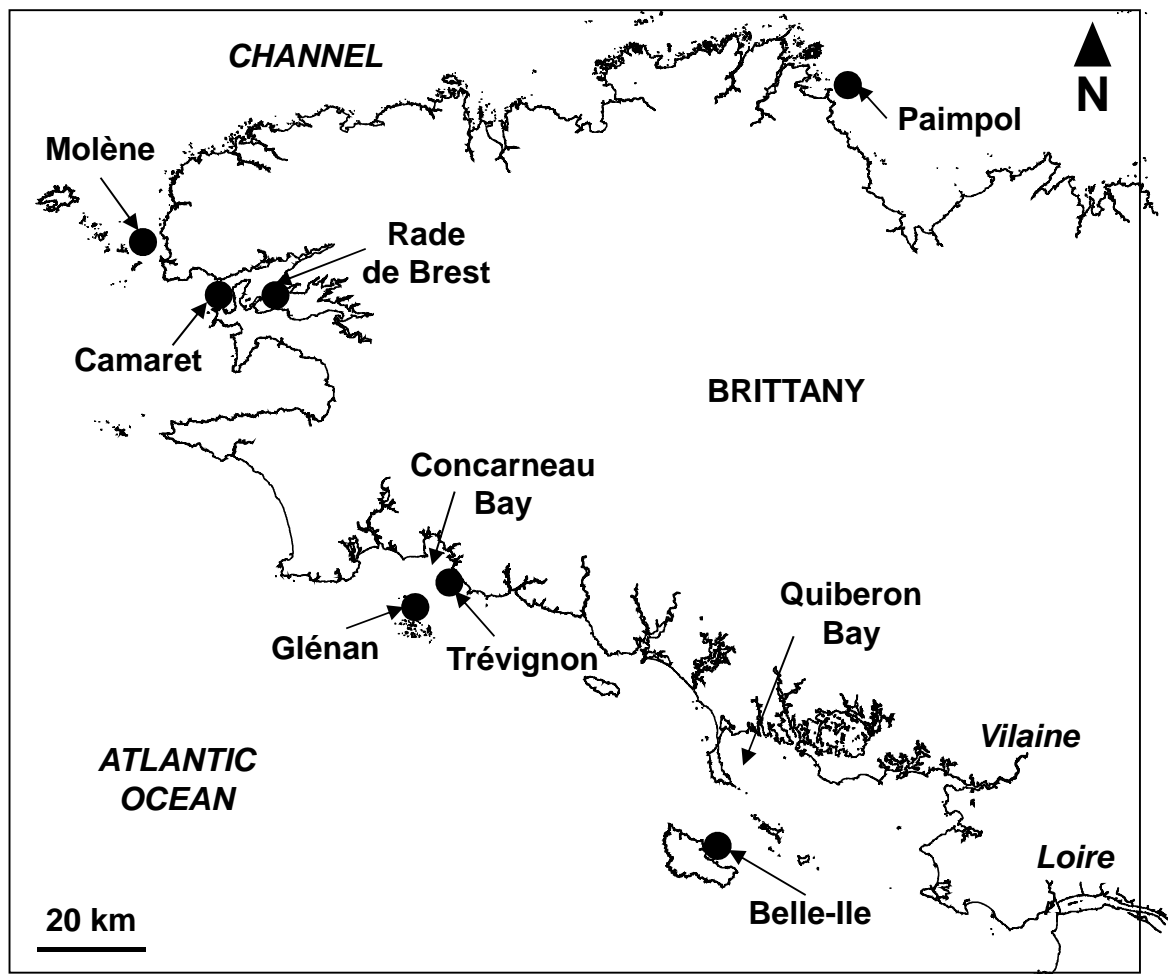
Maerl bed	Mud content (%)	Depth (m)	Current velocity (m.s ⁻¹)	Wave agitation (m.s ⁻¹)
Belle-Ile	0	10.0 - 17.9	0.20 max. = 0.34	0.62 max. = 3.56
Trévignon	1.0 - 2.0	1.9 - 15.8	0.02 - 0.06 max. = 0.18	0.36 - 0.37 max. = 2.86
Glénan	0	4.8 - 19.5	0.14 - 0.23 max. = 0.49	0.35 - 0.39 max. = 3.10
Camaret	0.4 - 21.2	13.6 - 20.8	0.07 - 0.31 max. = 0.44	0.14 - 0.36 max. = 5.50
Rade de Brest	2.7 - 46.6	0.7 - 6.8	0.08 - 0.26 max. = 0.43	0.01 - 0.09 max. = 3.57
Molène	0	7.0 - 12.6	0.26 max. = 1.52	0.22 - 0.39 max. = 2.57
Paimpol	0	10.8 - 25.9	0.59 - 0.73 max. = 1.71	0.19 - 0.27 max. = 1.87

754

755

756 Table 3. Physico-chemical properties of the water column generated near the bottom
 757 by three-dimensional numerical models for the maerl beds of the Brittany coast. For
 758 each environmental variable, annual mean value (bold characters) and annual range
 759 of variations are given.

Maerl bed	Temperature (°C)	Salinity	SPM concentration (mg.L ⁻¹)	Nitrate concentration (µM)	Oxygen saturation (%)
Belle-Ile	13.6 min. = 7.7 max. = 18.5	34.2 min. = 32.8 max. = 34.8	2.2 min. = 0.6 max. = 6.9	7.3 min. = 2.2 max. = 19.2	95 min. = 81 max. = 100
Trévignon	12.8 - 12.9 min. = 7.4 max. = 17.9	34.3 - 34.4 min. = 32.5 max. = 34.9	1.6 - 1.7 min. = 0.5 max. = 5.2	7.8 - 8.1 min. = 3.0 max. = 23.3	90 - 92 min. = 59 max. = 100
Glénan	13.3 min. = 7.7 max. = 17.6	34.5 min. = 33.0 max. = 35.1	1.7 - 1.8 min. = 0.6 max. = 5.4	6.7 - 6.8 min. = 2.9 max. = 19.5	94 min. = 74 max. = 100
Camaret	13.2 min. = 9.1 max. = 16.5	35.1 min. = 34.4 max. = 35.4	0.5 min. = 0.4 max. = 0.8	6.5 - 7.3 min. = 0.5 max. = 21.2	94 - 95 min. = 69 max. = 100
Rade de Brest	12.2 - 13.1 min. = 3.9 max. = 17.9	31.9 - 34.5 min. = 24.5 max. = 35.3	0.7 - 1.6 min. = 0.5 max. = 6.5	12.0 - 41.0 min. = 0.1 max. = 148.2	98 - 100 min. = 78 max. = 100
Molène	13.2 - 13.3 min. = 8.7 max. = 17.4	34.8 min. = 34.1 max. = 35.2	1.2 min. = 0.5 max. = 3.1	5.5 - 6.1 min. = 3.0 max. = 18.0	98 min. = 91 max. = 100
Paimpol	13.1 - 13.2 min. = 7.8 max. = 17.9	35.3 min. = 35.2 max. = 35.4	0.9 - 1.2 min. = 0.5 max. = 2.4	3.3 min. = 0.2 max. = 8.1	99 min. = 97 max. = 100

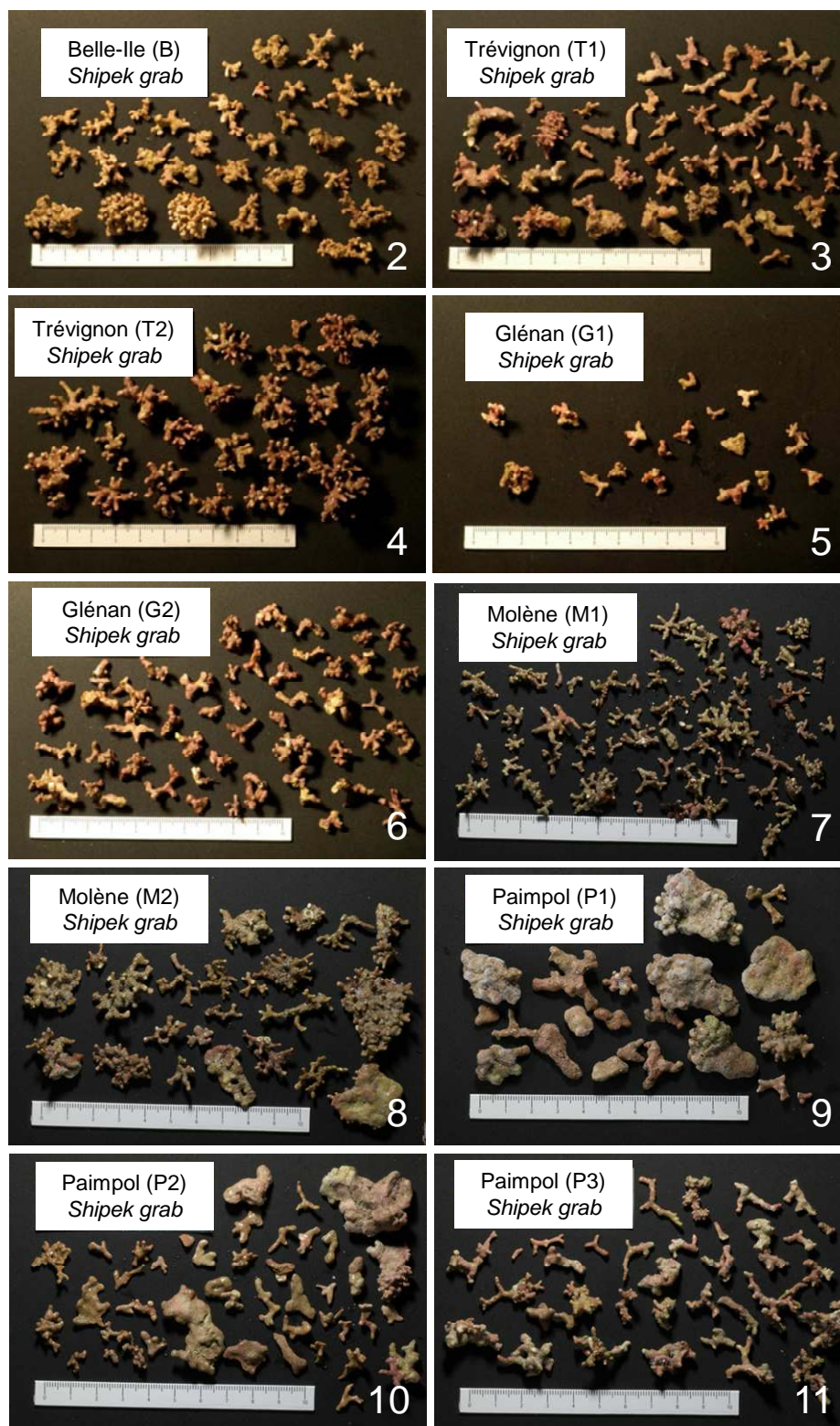


761

762 Figure 1. Location of the seven Brittany maerl beds studied by IFREMER (Paimpol,

763 Molène, Glénan, Trévignon and Belle-Ile) and IUEM (Rade de Brest and Camaret).

764

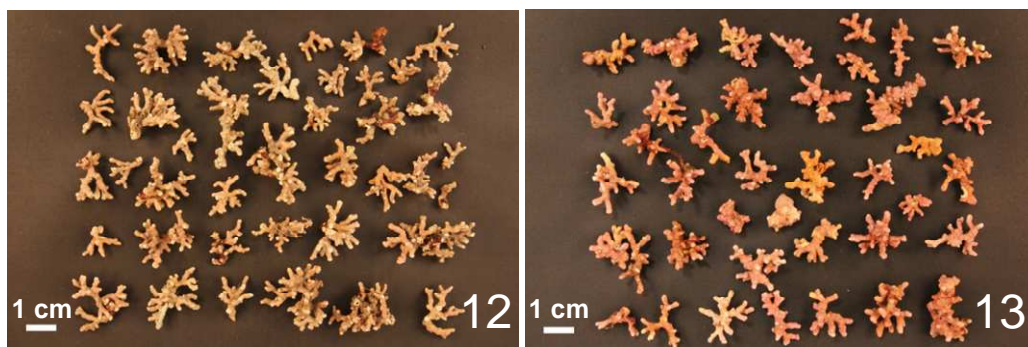


765

766 Figures 2-11. Examples of thallus morphology found within the subareas of the maerl

767 beds of Belle-Ile (B), Trévignon (T1 and T2), Glénan (G1 and G2), Molène (M1 and

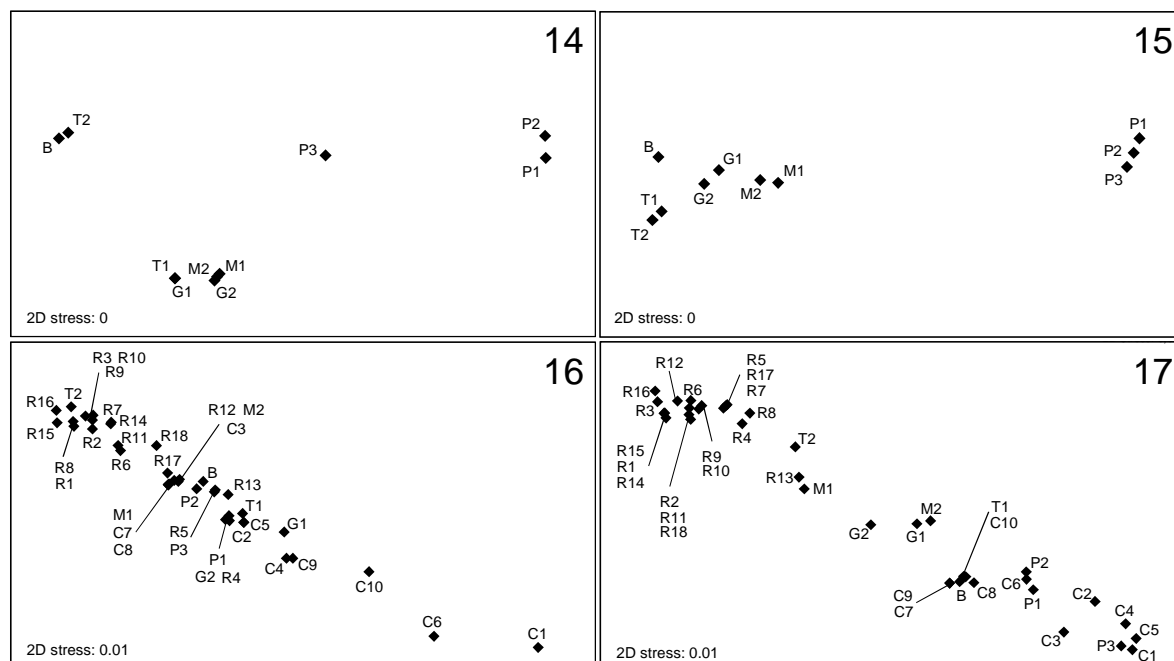
768 M2) and Paimpol (P1, P2 and P3).



769

770 Figures 12-13. Examples of thallus morphology found within the Smith-McIntyre grab
771 samples collected within the maerl beds of Rade de Brest (subarea R15, Figure 12)
772 and Camaret (subarea C2, Figure 13).

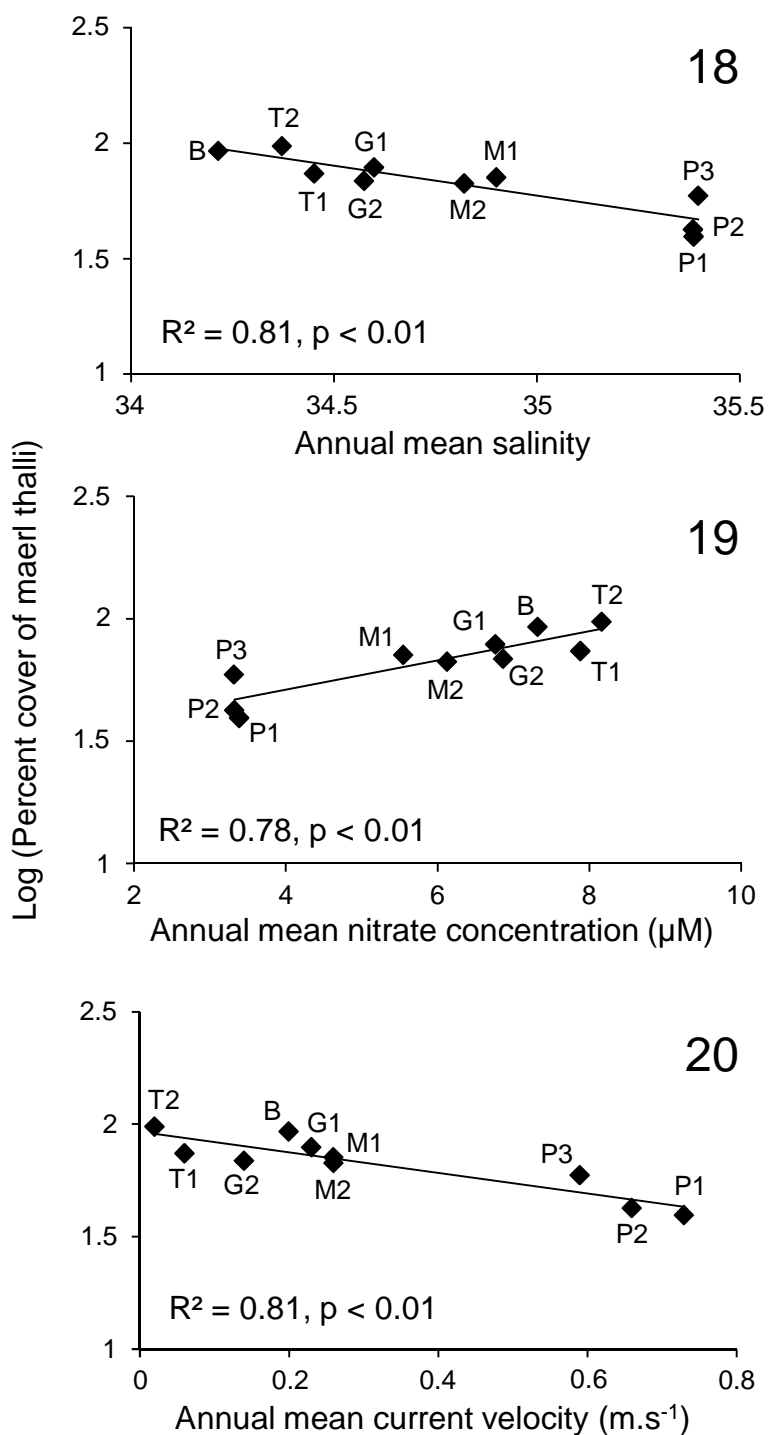
773



774

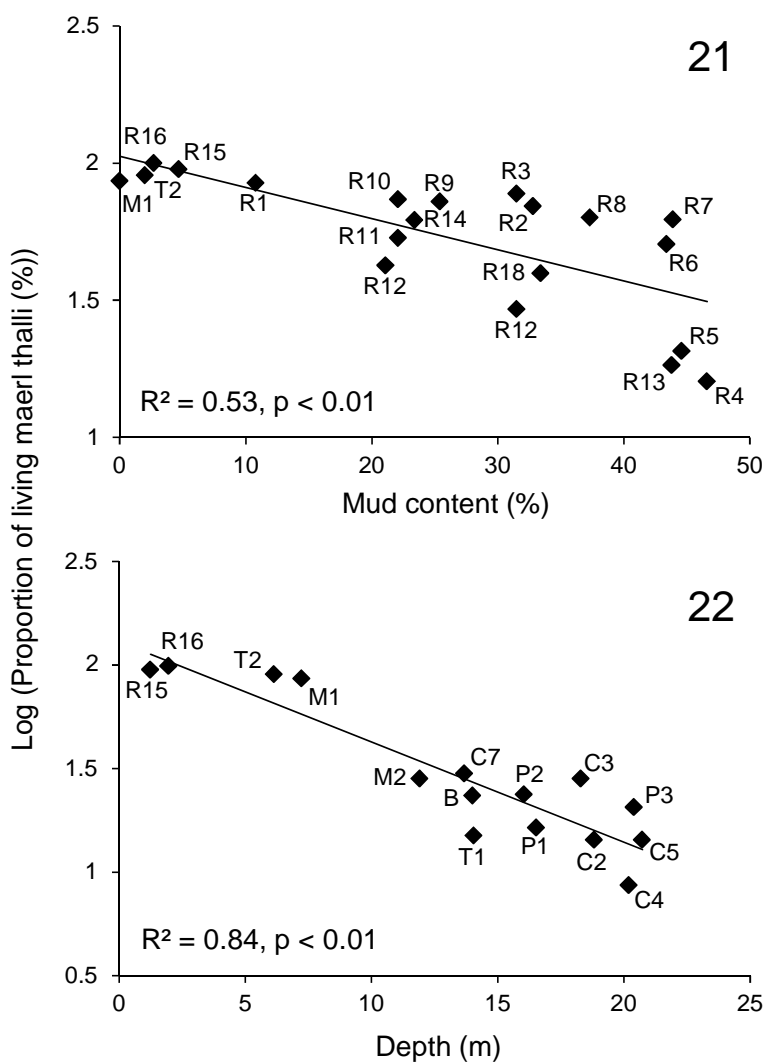
775 Figures 14-17. Nonmetric multidimensional scaling (NMDS) ordinations of the
 776 subareas of the Brittany maerl beds (Belle-Ile (B), Trévignon (T1 - T2), Glénan (G1 -
 777 G2), Camaret (C1 - C10), Rade de Brest (R1 - R18), Molène (M1 - M2), and Paimpol
 778 (P1 - P3)). NMDS ordinations are based on the percent cover of maerl thalli (Figure
 779 14) and the associated best subset of explanatory environmental variables (annual
 780 means of salinity, nitrate concentration and current velocity, Figure 15), and on the
 781 proportion of living thalli (Figure 16) and the associated best subset of explanatory
 782 environmental variables (depth and mud content, Figure 17).

783



784

785 Figures 18-20. Significant linear relationships ($p < 0.01$) between the percent cover of
 786 maerl thalli observed in the subareas of the Brittany maerl beds (Belle-Ile (B),
 787 Trévignon (T1 - T2), Glénan (G1 - G2), Molène (M1 - M2), and Paimpol (P1 - P3))
 788 and environmental variables (annual means of salinity, nitrate concentration and
 789 current velocity).



790

791 Figures 21-22. Significant linear relationships ($p < 0.01$) between the proportions of
 792 living thalli observed in the subareas of the Brittany maerl beds (Belle-Ile (B),
 793 Trévignon (T1 - T2), Camaret (C1 - C10), Rade de Brest (R1 - R18), Molène (M1 -
 794 M2), and Paimpol (P1 - P3)) and environmental variables (depth and mud content).
 795 The relationship with mud content was established for subareas situated at less than
 796 10 m of depth (Figure 21), while the relationship with depth was established for
 797 subareas showing less than 10 % of mud (Figure 22).

798

799